New insights into magnetic derivatives for structural mapping

Bruno Verduzco, University of Leeds, U.K.
J. Derek Fairhead and Chris M. Green, GETECH, Leeds, U.K.
Chris MacKenzie, BAFEX Exploration, Windhoek, Namibia

Magnetic and gravity derivatives can be likened to seismic attributes in that they can help define/estimate the physical properties of the source structure causing the anomaly. This contribution looks at the *tilt derivative*, first reported in 1994 and more recently used to derive the local wavenumber (1997). We will show that the combination of the tilt derivative and its *total horizontal derivative* are highly suitable for mapping shallow basement structure and mineral exploration targets and that they have distinct advantages over many conventional derivatives. We provide the simple theory behind the derivatives, use a range of simple 2D models to illustrate their response, and apply them to mapping a mineral target in Namibia.

Tilt derivative (TDR). The physical properties of a magnetic source structure that can be determined from a grid of magnetic data include its shape (plan), location of its edges, depth to top edges, dip, and rock susceptibility contrast. This contribution will focus on the first two—i.e. shape and edge detection. The problems to be overcome in data enhancement are to identify and map (a) subtle anomalies attenuated in the dynamic range due to the presence of high amplitude magnetic anomalies, (b) the continuity of individual bodies where there are lateral changes in susceptibility and/or depth of burial, and (c) the edges of structures by adequately accounting for the nature of the rock magnetization. Rock magnetization is a vector quantity that can consist of both remanent and geomagnetically induced components. The presence of the remanent component can adversely affect the shape of the magnetic field response and result in spurious derivatives, if one has assumed that only the induced component is present. Fortunately, basement rocks are usually dominated by the induced component, whereas mineralized zones often host long-lived remanent components. The following theory and 2D model examples show how these three problems can be successfully overcome, thus generating maps that can provide more reliable descriptions of source body parameters.

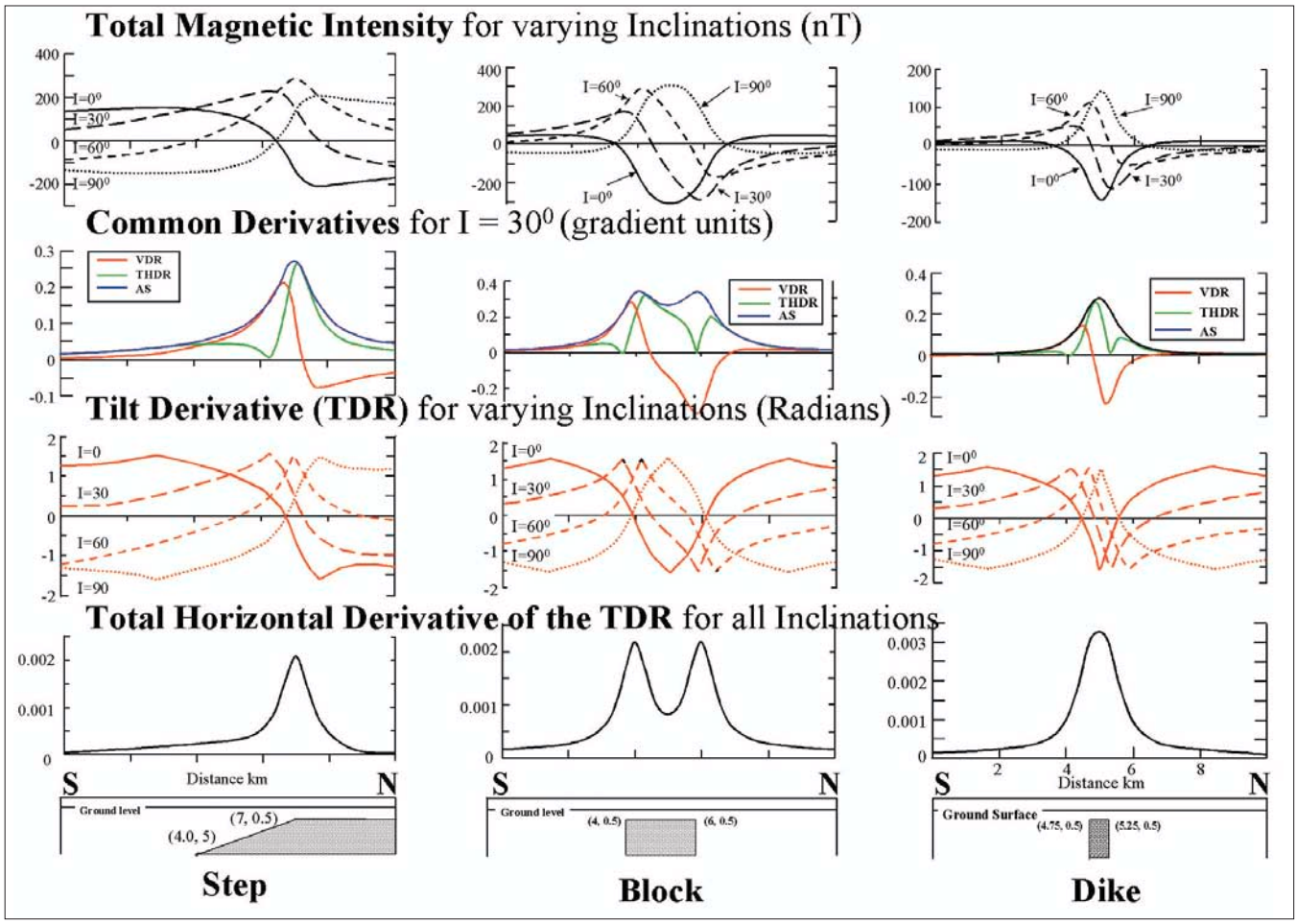

Figure 1. *Magnetic responses along S-N profiles across W-E striking 2D step, block, and dike models.*

The complex analytic signal for 2D structures is

$$A(x,z) = |A|\exp(j\theta)$$

where $|A| = \sqrt{\left(\frac{\partial T}{\partial x}\right)^2 + \left(\frac{\partial T}{\partial z}\right)^2}$ is known as analytic signal (AS), T is the magnitude of the total magnetic intensity (TMI), and $\theta = \tan^{-1}\left[\frac{\partial T}{\partial z} \Big/ \frac{\partial T}{\partial x}\right]$ is the local phase.

The tilt derivative is similar to the local phase, but uses the absolute value of the horizontal derivative in the denominator

$$TDR = \tan^{-1}\left[\frac{VDR}{THDR}\right]$$

where VDR and THDR are the first vertical and total horizontal derivatives, respectively, of the TMI. While VDR can be positive or negative, THDR is always positive. For profiles in the x direction,

$$THDR = \sqrt{\left(\frac{\partial T}{\partial x}\right)^2}$$

and for grids

$$THDR = \sqrt{\left(\frac{\partial T}{\partial x}\right)^2 + \left(\frac{\partial T}{\partial y}\right)^2}.$$

Due to the nature of the arctan trigonometric function, all amplitudes are restricted to values between $+\pi/2$ and $-\pi/2$ (+90° and -90°) regardless of the amplitudes of VDR or THDR. This fact makes this relationship function like an automatic gain control (AGC) filter and tends to equalize the amplitude output of TMI anomalies across a grid or along a profile.

The total horizontal derivative of TDR is

$$TDR\_THDR = \left|\frac{\partial TDR}{\partial x}\right|$$

for a profile and

$$TDR\_THDR = \sqrt{\left(\frac{\partial TDR}{\partial x}\right)^2 + \left(\frac{\partial TDR}{\partial y}\right)^2}$$

for a grid. These are equivalent to the absolute value of the local wavenumber.

These derivatives are applied in Figure 1 to simple 2D models (step, block, and dike) for a range of geomagnetic field inclinations (0, 30, 60, and 90°).

The important features to note from these models in Figure 1 are:

- AS is invariant for all inclinations (second panel from top) whereas conventional derivatives (VDR and THDR) are not. VDR and THDR are drawn for inclination = 30° only.
- The tilt derivatives vary markedly with inclination within an amplitude range of $\pm\pi/2$. For inclinations of 0 and 90°, the zero crossing is close to the edges of the model structures.
- The total horizontal derivative of TDR is independent of inclination, similar to AS. The difference between these derivatives is that the former is sharper and generates better defined maxima centered over the body edges, which persist to narrower features before coalescing into a single peak as shown in the dike model.

Not shown in Figure 1 is the fact that the amplitude response of all conventional derivatives (VDR, THDR, and AS) is closely linked to the amplitude of the TMI anomaly. On the other hand, the tilt derivative and, by association, its total horizontal derivative are independent of the amplitude of the TMI anomaly and are controlled more by the reciprocal of the depths to the sources which in the study area are small. These features are best illustrated in profile form in Figure 2 using observed data taken from Figure 3.

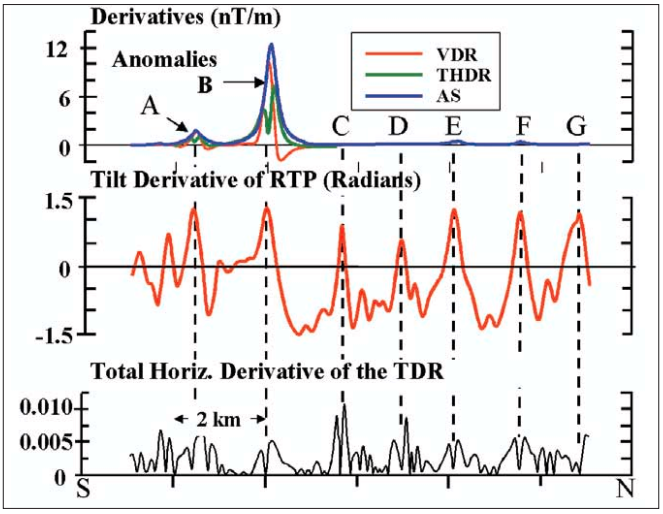

Figure 2. Profile P[1] (for location see Figure 3D) comparing the response of common derivatives to both the tilt and total horizontal derivative of the TDR.

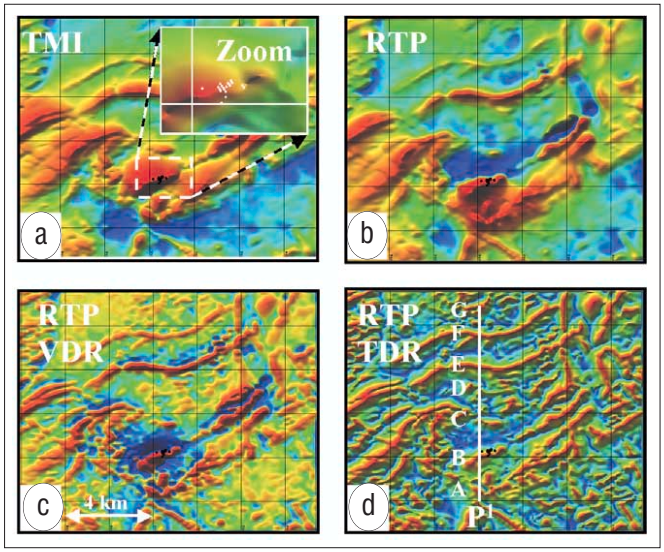

Figure 3. Color-equalized images (red high, blue low) for (a) total magnetic intensity, (b) reduced-to-pole, (c) vertical derivative of the RTP and (d) tilt derivative of the RTP.

The tilt derivative of the reduced-to-pole (RTP) field shows seven symmetric anomalies with highly variable TMI amplitudes. This symmetry is also seen in the TDR block and dike models (Figure 1) for I = 0° and I = 90°. Although reduced-to-pole and equator transformations work well, the RTP field is preferred because it preserves the imaging of N-S structures. In simple terms, the tilt derivative is acting like a very effective AGC filter. It also appears to act as an effective signal discriminator in the presence of noise (apart from the unlikely case when the noise has a similar spectral content to the signal).

The total horizontal derivative of the TDR preserves this amplitude enhancement in its ability to define edges by well-defined maxima (bottom panel of Figure 2). Since we have removed the directional component of the horizontal derivative, both the tilt and its total horizontal derivatives are easy to compute and plot. The advantages are threefold:

1) the tilt derivative has its zero values close to the edges of

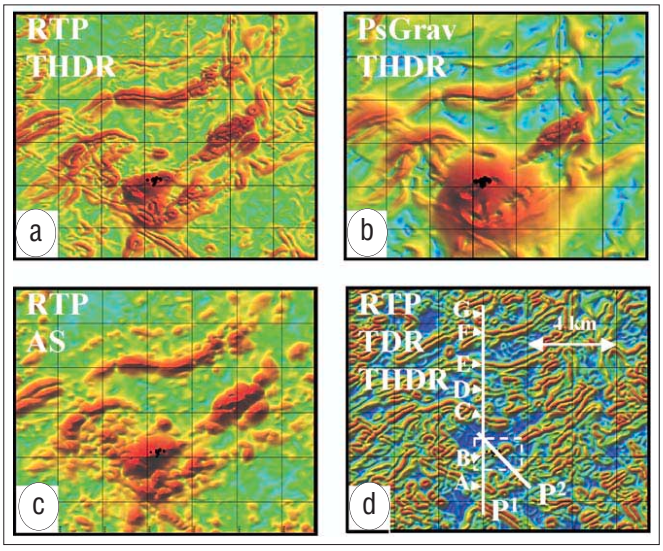

Figure 4. Color-equalized images of total horizontal derivatives of the RTP (a) and the pseudogravity (b), the analytic signal of the RTP (c) and the total horizontal derivatives of the tilt derivative after RTP (d). Location of profiles P^1 and P^2 are shown in (d).

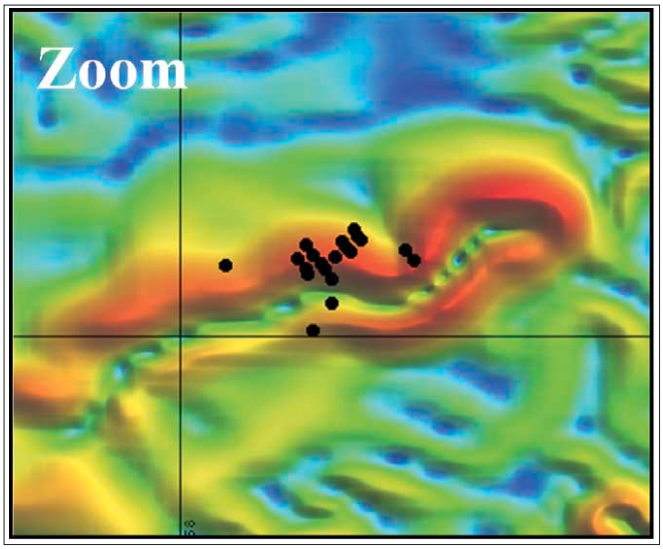

Figure 5. Zoomed-in area of white dashed box in Figure 4d showing the relationship between the location of the drill holes and the maxima of the RTP_TDR_THDR which is interpreted as defining the extent and edges of the causative magnetic body.

the body for RTP and RTE fields,
2) its phase is controlled by the vertical derivative
3) the "AGC" allows it to out perform the vertical derivative of the RTP (see Figure 3).

The total horizontal derivative of TDR is theoretically independent of geomagnetic inclination and so will generate useful magnetic responses for bodies having induced or remanent magnetization, or a mixture of both.

Field examples. The field examples in Figures 3-7 are from a 12 × 14 km area in north-central Namibia (150 km NNW of Windhoek), containing the Erindi gold prospect that covers an area of 36 km^2. The prospect, in the southern central zone of the Damara Belt, contains Neoproterozoic to Paleozoic metasediments and granites which are generally covered by up to 10 m of soil and calcrete. The gold occurrences are mainly associated with metamorphosed magmatic intrusions within the marbles of the Swakop Group. Previous exploration within the prospect, using geochemical soil sampling and ground magnetics, had located a highly anomalous gold zone, which was subsequently drilled. This drilling intersected a number of high-grade gold zones (with a best intersection of 11 m grading 9.5 g/t Au); but, due to the thick cover and indistinct geochemical response, the geologic continuity of these zones was poorly understood. The drill holes are shown as an inset to Figure 3a and superimposed on the TMI aeromagnetic data. Drill results indicate the mineralized structures dip at approximately 60° to the SE and show veins of magnetite skarn and massive sulphides within the marble unit. Pyrrhotite, pyrite, and magnetite are the dominant ore minerals and, as such, are highly magnetic compared to the hosting Swakop marble.

The study was undertaken by one of the authors (BV) as part of his master's thesis and postmaster's research with GETECH. The aim was to investigate by geophysical means whether the original drilling program was optimum for assessing the mineralization of the prospect and whether further drilling should be recommended. The study involved traveling to Namibia to collect all necessary data from the Geological Survey and BAFEX and undertaking a GPS survey of the existing boreholes. The digital aeromagnetic data used in the study were from the new high-resolution national data sets flown in 2001 and 2003 for the Namibian Geological Survey.

The aeromagnetic survey specifications are: flight spacing = 200 m; flying height = 80 m; flight direction = N-S; and survey names = 2116AD and 2116BC.

The digital grid used had a cell size of 50 m. All grid-based processing used GETECH's GETgrid software and the 2D modeling used NGA's GM-SYS. The inset to Figure 3a shows the location of the existing exploration drill holes which lie close to the maximum of the large magnetic anomaly (~1600 nT) that dominates the area.

Figure 3 shows the TMI(a) and RTP(b), using I = -62^0 and D = -12^0, for the area and the vertical derivative of the RTP(c) and the tilt derivative of the RTP(d). An alternative to the VDR(c) could be a high-frequency band-pass-filtered version of the RTP, but this has the disadvantage of requiring careful setting of filter parameters and (like the VDR) does not preferentially amplify the small amplitude signals that are automatically amplified by the TDR(d). Thus the tilt derivative provides an effective substitute for both the vertical derivative and the high-frequency band pass residual anomaly. It more clearly images and enhances, by its ability to "AGC," the smaller amplitude features. This, in turn, improves the ability to map subtle basement fabric. Of particular note is the removal of the blue halo generated by the VDR (Figure 3c) in the vicinity of the large anomaly and its replacement by a more evenly modulated field in Figure 3d. Superimposed on Figure 3d is the N-S profile P1 and the identification of the anomalies marked A-G in Figure 2.

Mapping the edges of structures can be achieved by a variety of methods as shown in Figure 4. The methods shown in Figures 4a-4c do not define edges as well as the total horizontal derivative of the TDR (Figure 4d). In Figure 4 we have generated both the AS (Figure 4c) and the total horizontal derivatives from the RTP field since the maxima over the edges of the same structure tend to generate more similar anomaly amplitudes than using the TMI field. The role of other derivatives in any interpretation should not be overlooked. AS (Figure 4c) is a good spatial indicator of susceptibility contrast and pseudo gravity (Figure 4b) helps define the possible extent of the mineralization.

To investigate the relation between structure, the drilling results and the mineralization, Figure 5 provides a zoomed-in view of part of the prospect (dashed white box in Figure

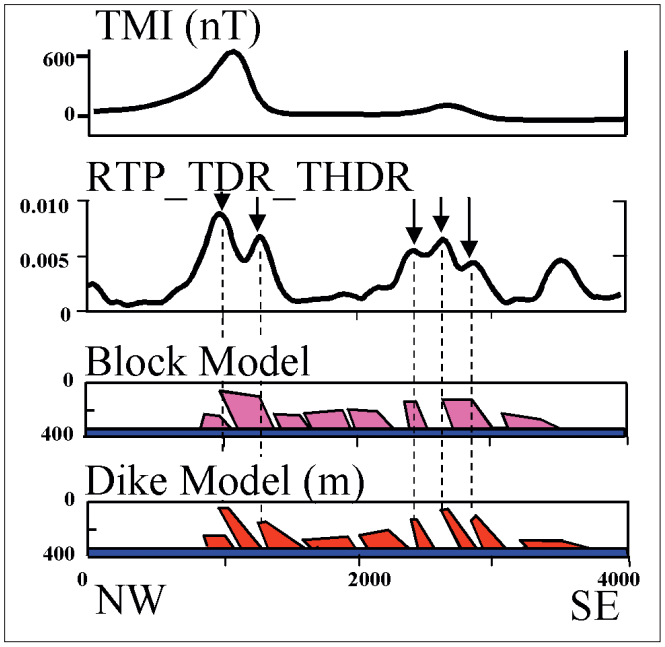

Figure 6. *Interpretation of profile P2 (location shown in Figure 4d) passing through the drill holes and intersecting the ENE-WSW trending structure (see Figure 5) to the ENE of the TMI magnetic maximum. Models assuming either blocks or dikes as the cause of the main anomalies (identified by arrows and dashed lines) are shown. Susceptibility contrast between the blocks (and dikes) and the background marble units reaches 0.02 cgs.*

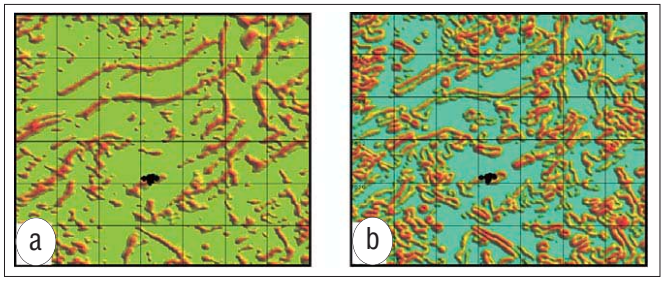

Figure 7. *(a) The tilt derivative with all values less than 0.0 replaced by 0.0. This shows the approximate width and distribution of features with positive susceptibility. (b) The RTP_TDR_THDR with depth threshold cut-off set to visualize only shallow structures with positive or negative susceptibilities.*

4d). This reveals that the drill holes tend to be located over and to the north of the main contact and have probably not intersected sufficiently the main magnetic body delineated by the maxima. Since the anomalies could represent either a series of dipping thick sheets (blocks) or dike features, both interpretations are shown in the interpreted profile P2 for the main anomalies passing through the drill hole locations (Figure 6). For both model types a closely spaced set of thin sheets (not shown) could equally result in a similar set of anomalies.

Conclusion. This contribution shows that it is relatively simple with existing potential field data to construct "AGC" images by means of the tilt derivative of RTP, which provides an effective alternative to the vertical derivative to map continuity of structures and enhance magnetic fabric. The advantages of the tilt derivative are its abilities to normalize a magnetic field image and to discriminate between signal and noise. Since the zero crossing of the tilt derivative is close to the edge of the structure for RTP and RTE data, then applying a threshold cutoff of 0.0 in Figure 7a isolates all bodies with positive susceptibility contrast.

The enhanced amplitudes of the tilt derivative can be carried through to its total horizontal derivative (or local wavenumber) in which the edge anomalies prominent and invariant to geomagnetic inclination, thus making this derivative effective for mapping geologic edges. This study has not encountered the problem of multiple maxima (ringing) that generates false edges. Further, since the depth to top is inversely related to amplitude of the total horizontal derivative for contacts, a threshold cutoff can be set to act as an effective depth discriminator that will isolate shallow sources. This makes structural mapping more intuitive (Figure 7b).

Finally, the derivatives shown here are some among many which can be used in different ways, depending on the geologic setting, to help map basement structure. In this study, we have provided a geophysical means of reassessing existing exploration drilling results over shallow basement cover and a basis for planning new drilling programs. The results of the study indicate that the main magnetic target has not previously been sufficiently drill tested and that good potential exists to discover further gold mineralization in the vicinity of the TDR-defined anomalies.

Suggested reading. "Potential field tilt—A new concept for location of potential field sources" by Miller and Singh (*Journal of Applied Geophysics*, 1994). "Automatic conversion of magnetic data to depth, dip, and susceptibility contrast using the SPI method" by Thurston and Smith (GEOPHYSICS, 1997). TLE

Acknowledgments: We thank Dave Hutchins and Godfrey Ngaisiue of the Namibian Geological Survey and BAFEX Exploration for their support in making the study possible. We also thank Mark Pilkington for helpful discussions and to Jeffrey Phillips for reviewing the manuscript.

Corresponding author: jdf@getech.com